ISOMAse
International Society of Ocean, Mechanical and Aerospace Scientists and Engineers

Journal of Ocean, Mechanical and Aerospace
-Science and Engineering-
30th July 2024. Vol.68 No.2

July 30, 2024

Numerical Analysis of Sedimentation in Open Channels Using Computational Fluid Dynamics

Yoga Satria Putra[a,*], Evi Noviani[b], Hasanuddin[c], Elsa Kurnia[a] and Maria Citra Puella Christy[a]

[a)] *Department of Geophysics, Faculty of Mathematics and Natural Science, Tanjungpura University, Indonesia*
[b)] *Department of Mathematics, Faculty of Mathematics and Natural Science, Tanjungpura University, Indonesia*
[c)] *Department of Physics, Faculty of Mathematics and Natural Science, Tanjungpura University, Indonesia*

*Corresponding author: yogasatriaputra@physics.untan.ac.id

Paper History

Received: 18-May-2024
Received in revised form: 16-July-2024
Accepted: 30-July-2024

ABSTRACT

This study investigates sedimentation in open channels utilizing Computational Fluid Dynamics (CFD). The validation indicates a strong agreement between the simulation and the reference data. Flow velocity substantially decreases in the branched channel post-bifurcation. Similarly, at a 90° bend, there is a notable drop in flow velocity after the curve. A vortex forms in areas where the velocity decreases. Sedimentation prediction can be achieved by observing these velocity reductions in specific channel sections. In the branched channel, low velocities and localized water eddies are found after the bifurcation point. In a channel with a 90° bend, the velocity diminishes on the inner side of the curve, with vortices forming, acting as potential sediment traps. This study highlights the utility of CFD as an effective method for enhancing the understanding of sedimentation processes in river systems.

KEYWORDS: *CFD, open channel flow, sedimentation, flow velocity*

NOMENCLATURE

P	Pressure
t	Time
$\boldsymbol{u}$	Velocity Vector
v	Initial Flow Velocity
v_*	Velocity Near the Bottom of the Channel
W	Channel Width
z_0	Depth Near the Stream Bed
α	Dip-Correction Parameter
h	Initial Depth of Flow
κ	Von Karman Constant (= 0.41)
l	Sub-Channel Length
μ	Fluid Kinematic Viscosity
∇	Divergence Operator
ρ	Fluid Density
ξ	Normalized Distance of Flow Depth
Δx	Grid Size, x-component
Δy	Grid Size, y-component
Δz	Grid Size, z-component
C	Volume Fraction of Fluid
H	Channel Height
L	Channel Length
CFD	Computational Fluid Dynamics
DMLW-law	Dip-Modified Log-Wake Law
FVM	Finite Volume Method
OpenFOAM	Open Field Operation and Manipulation
RANS	Reynolds-Averaged Navier-Stokes
VoF	Volume of Fluid

1.0 INTRODUCTION

Sedimentation poses a significant challenge in river and watershed management as it can obstruct water flow, alter riverbed topography, and impact aquatic ecosystems. Studying sedimentation is crucial to developing solutions for these issues. Sedimentation, the process where solid particles settle in flowing water or other fluids, is fundamental to both aquatic ecosystems and human infrastructure. This phenomenon occurs in open channels such as rivers, ditches, and drainage systems. Sedimentation in these channels greatly affects various aspects of human life. Deposited sediment can lead to problems like river channel shallowing, which may cause flooding or degrade water quality by including dissolved particles. Managing sedimentation is particularly complex in river basins, necessitating a deep understanding of its mechanisms. This article delves into the sedimentation mechanisms in open channels, focusing on how channel geometry influences flow velocity changes. To address this issue, we employed

JOMAse | Received: 18-May-2024 | Accepted: 30-July-2924 | [(68) 2: 53-63]
Published by International Society of Ocean, Mechanical and Aerospace Scientists and Engineers, www.isomase.org., ISSN: 2354-7065 & e-ISSN: 2527-6085

Computational Fluid Dynamics (CFD) to offer a detailed analysis of the sedimentation process in open channels.

Numerous studies have analytically explored the fundamental properties of sediment in open channels. By employing theoretical and mathematical techniques, researchers have modeled sediment dynamics and identified the key parameters influencing the sedimentation process [1,2]. One such study predicted sediment transport in channel bends by incorporating the effects of channel geometry into the model [3]. Experimental research has also been conducted to understand sedimentation mechanisms in open channels, focusing on how physical conditions such as flow velocity, channel geometry, and sediment characteristics affect sediment deposition [4,5,6]. For instance, an experimental study examined sediment transport mechanisms in branching channels [7]. In addition to analytical and experimental approaches, several numerical studies have been undertaken. These include developing numerical models to analyze sediment transport in open channels [7,8,9,10] and simulating flow velocity in winding channels [11,12,13]. Recently, there has been a shift towards using Computational Fluid Dynamics (CFD) to model sedimentation in open channels. Two-dimensional numerical simulations employing the CFD/Discrete Element Method (CFD-DEM) have been used to study particle sedimentation in channels [14]. CFD models have also been utilized to simulate sediment deposition in water reservoirs [15,16], and Direct Numerical Simulation (DNS) has been applied to model turbulence in open channel flows related to sediment transport [17,18,19]. Various studies using the CFD approach have established a robust foundation for a more detailed exploration of sedimentation mechanisms in open channels [20,21,22].

Given the issues and prior research outlined earlier, it is crucial to study sedimentation mechanisms in open channels. This research aims to analyze these mechanisms using a CFD approach, focusing on how channel geometry affects flow velocity changes. To enhance the reliability of the simulation, an initial validation stage was conducted by comparing the water velocity distribution profile in a straight channel between the simulation results and the experimental and numerical findings of Alawadi et al. (2019) [23]. The simulation utilized the open-source software OpenFOAM, employing the Reynolds-averaged Navier-Stokes (RANS) k-Epsilon turbulence model to address turbulence at the channel walls and bottom. Two types of channel geometries branched channels and 90-degree curved channels were constructed to study the impact of geometry on flow velocity changes. A decrease in velocity in certain channel sections indicates sedimentation in those areas. This research aims to contribute to a better understanding of sedimentation mechanisms in open channels such as rivers, irrigation systems, and ditches. Understanding these mechanisms is essential for advancing watershed management technology.

2.0 METHODOLOGY

This study employed numerical methods to create a 3D simulation of water flow in an open canal using the open-source software OpenFOAM, incorporating the RANS k-Epsilon turbulent model. The simulation took place at the Laboratory of Geophysics and Geographic Information Systems (GIS), Universitas Tanjungpura, Pontianak, West Kalimantan. The research was conducted through several stages, including a review of existing literature, the creation of a computational domain using the free software Salome 9.9.0, validation studies, flow modeling in open channels using OpenFOAM, and analysis of simulation outcomes using the free software Paraview version 5.8.0.

2.1 Resources and Equipment

The materials utilized in this study comprise secondary data, specifically the vertical velocity distribution profile of water flow in a straight channel. This secondary data includes experimental and analytical findings from Alawadi et al. (2019) [23]. The velocity profile data will be employed to contrast the flow velocity profiles derived from simulations conducted with OpenFOAM. The research equipment encompasses both hardware and software components, detailed in Table 1. All software utilized in this study is freely available and open-source, as outlined in Table 1.

Table 1: Instruments used in the study

No	Tools	Specification
1	Laptop	Intel(R) Core (TM) i7-1165G7 @ 2.80GHz 2.80 GHz, RAM: 16,0 GB
2	Open-Source OpenFOAM Software	Versi OpenFOAM-dev
3	ParaView	Versi 5.8.0
4	WebPlotDigitizer	Versi Online
5	Operating system	Ubuntu 22.04 LTS
6	External Hardisk	6 TB
7	Salome	Versi 9.9.0
8	Gnuplot	Versi 6.0

2.2 Computational domain

This study commences by establishing computational domains for open channels. Two types of computational domains are created: (1) domains for validation, featuring straight channels, and (2) domains for analyzing flow velocity changes, consisting of branched channels and 90° curved channels. The initial domain constructed is for validation purposes, representing a straight channel geometry, depicted in Figure 1(a). This domain serves as a validation tool to compare simulated data against experimental and analytical data. Its dimensions replicate those of experiments conducted by Alawadi et al. (2019) [23], with length x width x height = L x W x H = 6 x 1 x 1 m (Figure 1(a)). The branched channel comprises a primary and secondary channel. The computational domain for the primary channel in the branched setup measures L x W x H = 8 x 1 x 1 m, while the secondary channel's domain dimensions are L x W x H = 1 x 1 x 1 m (Figure 1(b)). Similarly, the 90° curved channel consists of primary and secondary channels. The primary channel's computational domain in the curved setup is L x W x H = 7 x 1 x 1 m, while the secondary channel's dimensions are L x W x H = 6 x 1 x 1 m (Figure 1(c)). These channels, whether straight, branched, or curved, are bounded by six boundaries: inlet, top inlet, outlet, bottom, walls, and atmosphere. The computational domain construction and meshing processes are facilitated using Salome software version 9.9.0. All domains employ the

JOMAse | Received: 18-May-2024 | Accepted: 30-July-2924 | [(68) 2: 53-63]
Published by International Society of Ocean, Mechanical and Aerospace Scientists and Engineers, www.isomase.org., ISSN: 2354-7065 & e-ISSN: 2527-6085

ISOMAse
International Society of Ocean, Mechanical and Aerospace Scientists and Engineers
Journal of Ocean, Mechanical and Aerospace
-Science and Engineering-
30th July 2024. Vol.68 No.2

July 30, 2024

"tetrahedral" mesh type with the Netgen 1D-2D-3D algorithm. Mesh sizing is determined, with the maximum set at 0.01 m and the minimum at 0.005 m, utilizing a "fine" fineness type.

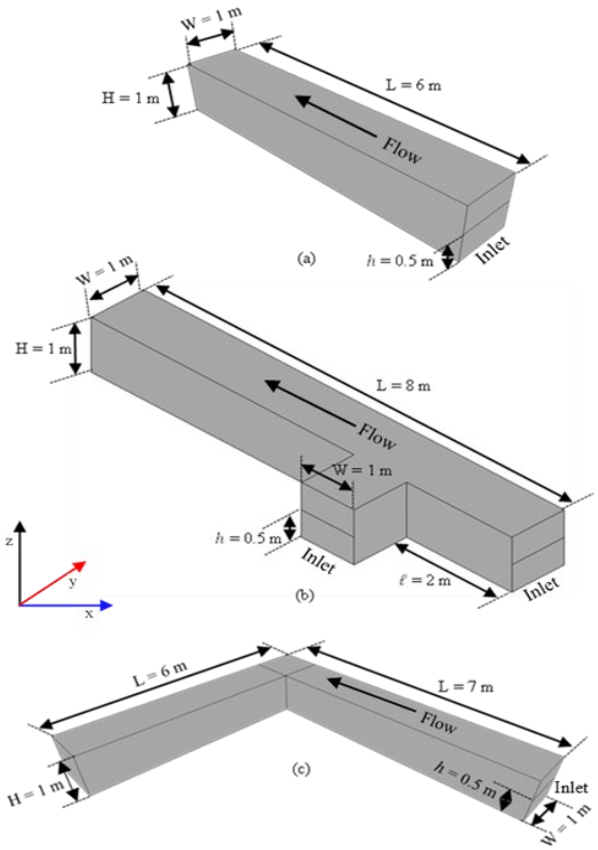

Figure 1: Three categories of computational domains: (a) linear channel, (b) divided channel, and (c) channel with a 90° bend

In the three channel types, Neumann boundary conditions are employed at the inlet, outlet, and atmosphere, facilitating water ingress and egress through these boundaries. Conversely, Dirichlet boundary conditions are imposed at the channel walls and bottom, where a specified value is established. At the inlets of all three channel types, an initial velocity of v_0 = 0.5 m/s and an initial water depth of h = 0.5 m are set. To address turbulence at the boundaries of the canal's walls and bottom, the RANS k-Epsilon turbulent model is utilized, configured within the "momentumTransport" file. Additionally, the fluid's physical property values for this simulation are detailed in Table 2.

Table 2: Characteristics of water

No	Physical properties	Constant
1	Surface tension	0,07 N/m
2	Gravitational acceleration	-9,81 (m/s^2)
3	Air density	1 kg/m^3
4	Water kinematic viscosity	1 x 10^{-6} m^2/s
5	Water density	1000 kg/m^3
6	Air kinematic viscosity	1,48 x 10-5 m^2/s

2.3 Flow model

The computational tool employed in this simulation is the "interFoam" solver, designed to address the Navier-Stokes equations involving two-phase flow of water and air. These equations, serving as the foundation for the flow model in the simulation, are articulated through continuity and momentum equations.

$$\nabla \cdot \mathbf{u} = 0 \tag{1}$$

$$\rho\left(\frac{\partial \mathbf{u}}{\partial t} + \mathbf{u} \cdot \nabla \mathbf{u}\right) = -\nabla P + \mu \nabla^2 \mathbf{u} + \mathbf{f} \tag{2}$$

where $\nabla \cdot \mathbf{u}$ is the divergence of the velocity vector $\mathbf{u}$. The forms $\frac{\partial \mathbf{u}}{\partial t}$, $\mathbf{u} \cdot \nabla \mathbf{u}$, ∇P, $\nabla^2 \mathbf{u}$, ρ, μ, and $\mathbf{f}$ are variations in velocity over time, convective momentum, pressure gradients, velocity Laplacian, fluid density, fluid kinematic viscosity, and external forces exerted on the fluid are all considered. The "interFoam" solver employs the Finite Volume Method (FVM) to address equations (1) and (2).

For addressing two-phase flow involving water and air with a clear interface, the "interFoam" solver utilizes the Volume of Fluid (VoF) technique. This approach facilitates precise modeling by tracking the interface movement between the water and air phases during flow simulation. In OpenFOAM, the VoF method employs the volume fraction C, referred to as "alpha" in OpenFOAM, as an indicator function. This volume fraction C determines the proportion of the cell filled by the fluid, characterized by the following definition [24]:

$$\begin{cases} C(x,y,z,t) = 1 & \text{occupied by water,} \\ 0 < C(x,y,z,t) < 1 & \text{interface} \\ C(x,y,z,t) = 0 & \text{occupied by air} \end{cases} \tag{3}$$

Moreover, utilizing the formulation presented in equation (3), the Volume of Fluid (VoF) mass conservation method is employed to simulate the transition of volume from one phase to another throughout the simulation. The mass conservation equation can be expressed as follows:

$$\frac{\partial C}{\partial t} + \nabla \cdot (\mathbf{u}C) = 0 \tag{4}$$

where $\mathbf{u}$ and ∇ are the velocity vector of the flow and the operator for divergence, respectively.

2.4 Analytical of vertical velocity distribution

Numerous scholars have investigated the phenomenon of velocity reduction close to the flow surface. Some have suggested enhancements to the log and wake laws for better prediction of velocity reduction in open channel flows [23], [25,26,27,28]. In open channels, it is presumed that secondary flow and turbulence emerge due to the existence of a free surface, which notably affects velocity forecasts. An analytical model for velocity distribution, accounting for the decreasing velocity near the surface, has been formulated, known as the Dip-Modified Log-Wake law (DMLW-law) [29]:

$$\frac{U}{u_*} = \frac{1}{\kappa}\left[\ln\left(\frac{\xi}{\xi_0}\right) + \frac{2\Pi}{\kappa}\sin^2\left(\frac{\Pi}{2}\xi\right) + \alpha \ln(1-\xi)\right] \tag{5}$$

with U, u_*, κ, α, ξ, and ξ_0 are the mean flow velocity of

JOMAse | Received: 18-May-2024 | Accepted: 30-July-2924 | [(68) 2: 53-63]
Published by International Society of Ocean, Mechanical and Aerospace Scientists and Engineers, www.isomase.org., ISSN: 2354-7065 & e-ISSN: 2527-6085

water, velocity close to the channel bed, Von Karman constant, parameter for correcting dips that represent secondary flow impacts, and distance normalized with respect to flow depth h ($\xi = z/h$) respectively, and $\xi_0 = z_0/h$, where z_0 is the location close to the bottom of the flow depth. Meanwhile Π is described as the Coles parameter indicating the turbulence intensity of a flow impacting a surface [30].

3.0 RESULTS AND DISCUSSION

3.1 Validation Study

At the outset of this discussion, a validation analysis was conducted to assess the precision of the computational fluid dynamics (CFD) simulation outcomes concerning water flow in open channels, utilizing the OpenFOAM software. Figure 2 depicts the outcomes of a 3D simulation illustrating water flow in a linear channel, along with a top-view showcasing velocity distributions at two depths: near the surface (h = 0.45 m) and near the channel bed (h = 0.05 m). These visualizations reveal that the slowest velocities are observed adjacent to the channel walls.

In Figure 2(a), the 3D simulation illustrates that water velocity follows the typical flow pattern in an open channel, with the highest velocities occurring at the center and the lowest near the walls, indicative of wall friction-induced velocity reduction. Figures 2(b) and 2(c) provide additional insight by presenting velocity distributions at different depths. Even at a shallow depth near the surface (h = 0.45 m), Figure 2(b) illustrates reduced flow velocity near the channel walls. This trend persists at a depth close to the channel bed (h = 0.05 m), as shown in Figure 2(c), underscoring the enduring impact of wall friction, even in proximity to the bottom.

Figure 3 juxtaposes the vertical velocity distribution profile obtained from the OpenFOAM simulation with experimental and analytical findings [23]. The vertical distribution highlights that the lowest velocity is typically observed near the channel bed, aligning with the expected velocity distribution in open channels. Recent research has suggested a velocity decrease (referred to as a velocity-dip) near the free surface [23]. The simulations utilizing this CFD method demonstrate consistency with the velocity-dip phenomenon depicted in the velocity distribution profile, corroborating the experimental and analytical findings. This graphical representation provides further support for the accuracy of the simulation outcomes. The curve pattern closely mirrors that of the experimental and analytical results, underscoring the CFD model's capability to replicate natural velocity distributions. An accurate comprehension of velocity changes in open channels aids in predicting sediment movement within these flows. Moreover, adherence to scientific principles in velocity distribution enhances the CFD's capacity to depict water flow in real-world channels.

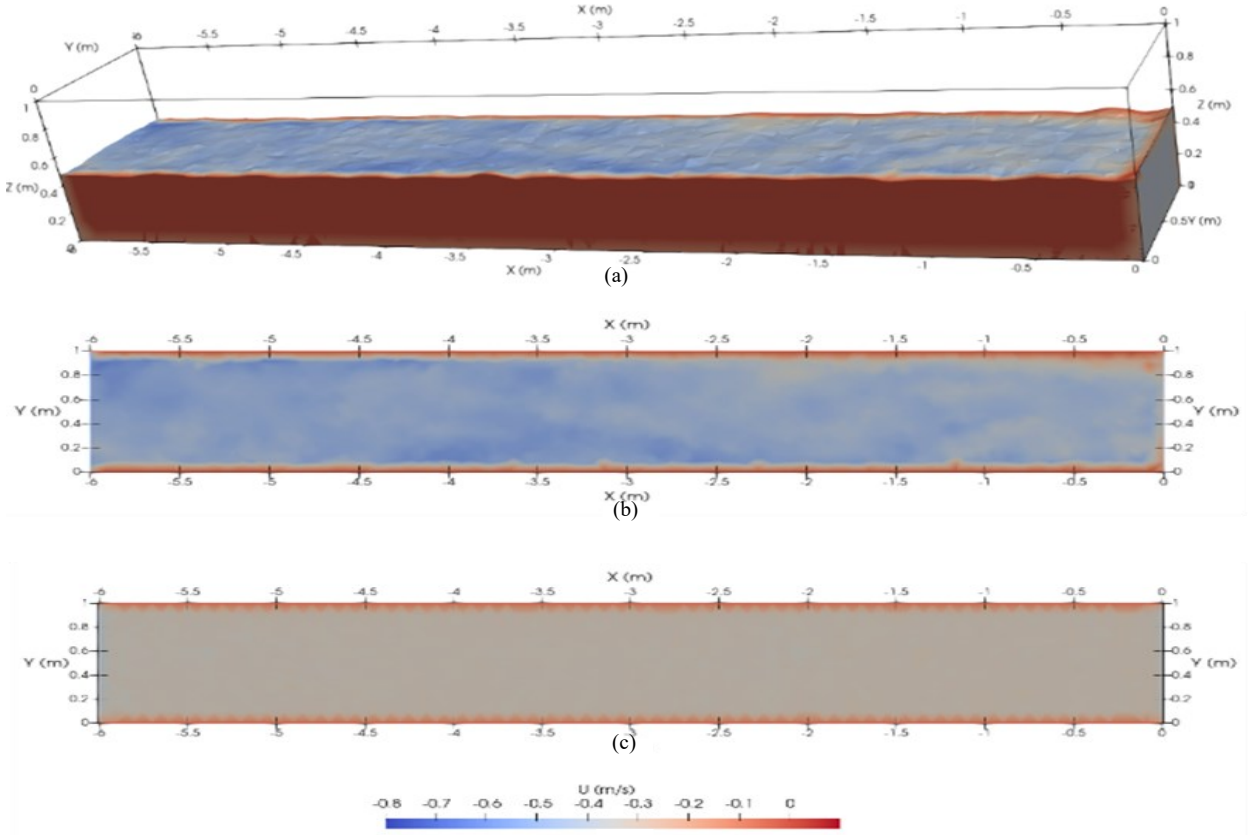

Figure 2: (a) 3D simulation depicting water flow in a linear channel; A bird's-eye view of velocity distributions in a linear channel: (b) depth close to the surface at h = 0.45 m, and (c) depth near the channel bed at h = 0.05 m

JOMAse | Received: 18-May-2024 | Accepted: 30-July-2924 | [(68) 2: 53-63]
Published by International Society of Ocean, Mechanical and Aerospace Scientists and Engineers, www.isomase.org., ISSN: 2354-7065 & e-ISSN: 2527-6085

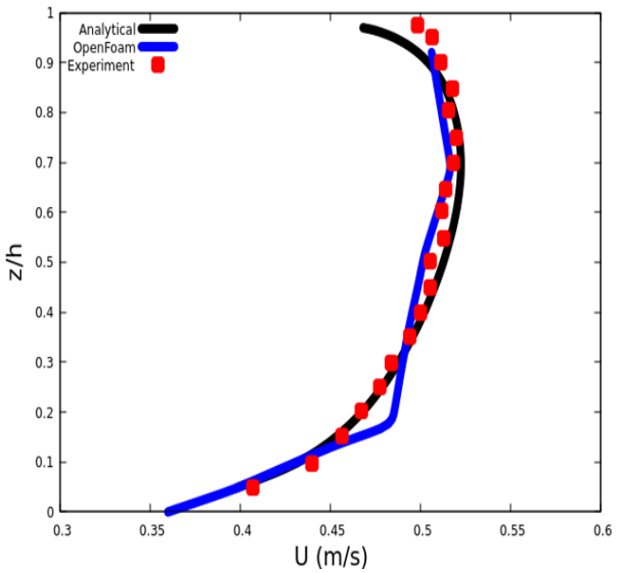

Figure 3: The vertical distribution profiles of water velocity from the OpenFOAM simulation are compared with experimental and analytical results (Eqn. (5))

3.2 Changes in Velocity within Branched Channels

In this section, the outcomes of 3D simulations depicting water flow in branched channels are presented, as illustrated in Figure 4(a). This visually depicts the flow pattern within branched channels. A reduction in velocity is observed in the flow subsequent to the point of branching between the two channels. This aligns with the scientific principle that when the flow undergoes constriction following the convergence of channel branches, its velocity diminishes. This is a consequence of the continuity principle, which dictates that a narrower stream will exhibit a reduced velocity to uphold the same flow rate.

Figure 4(a) is sliced using Paraview to visualize the velocity fields at two distinct depths: close to the surface at h = 0.45 and near the channel bottom at h = 0.05 m, as depicted in Figure 4(b) and (c). These findings offer insights into how alterations in the geometry of branched channels can impact variations in water velocity. Figure 4(b) and (c) depict alterations in velocity at depths near the surface (h = 0.45 m) and close to the channel bed (h = 0.05 m), respectively. A reduction in velocity (referred to as velocity-dip) is evident at the surface, specifically at h = 0.45 m, indicating the impact of flow constriction on the upper layer. This phenomenon remains observable at depths near the channel bed, albeit possibly with slight variations in intensity. The interaction between the channel bed and the overlying water flow can lead to a decrease in velocity near the channel bottom. Recognizing the locations where velocity decreases is crucial for predicting sedimentation occurrences in an open channel. The decrease in velocity subsequent to a channel bifurcation can influence sediment settling within the flow. Heavier sediment particles may settle earlier in regions with lower velocities. Furthermore, the simulation results demonstrate that the CFD approach used to simulate flow in branched channels adheres to scientific principles. These findings instill confidence in the reliability of the CFD approach for further exploration of the influence of channel geometry on velocity alterations and sedimentation mechanisms.

3.3 Changes in Velocity within a 90° Curved Channel

Figure 5 depicts the outcomes of a 3D water flow simulation within a 90° curved channel conducted using OpenFOAM with the RANS k-Epsilon turbulent model. These visual findings reveal a notable occurrence in the water flow dynamics as it traverses this sharp curve. The flow within the 90-degree curved channel demonstrates a significant velocity reduction subsequent to passing through the bend. This reduction is consistent and can be attributed to the centrifugal force generated by the alteration in flow direction. Such centrifugal force leads to a decrease in flow velocity, particularly on the inner side of the bend within the indicated area (yellow box). This phenomenon aligns with fundamental principles in fluid mechanics, which stipulate that liquid flow experiences a velocity decrease when encountering a sharp bend.

The outcomes of the simulation depicted in Figure 7 carry significant implications for comprehending flow dynamics in channels featuring sharp bends. A reduction in flow velocity within this segment can influence sediment behavior within the channel, potentially leading to sediment deposition and affecting sediment distribution and accumulation. Consequently, a thorough understanding of this phenomenon holds considerable importance in the realm of sedimentation mechanisms. In summary, these simulation results offer valuable insights into the flow dynamics within a channel characterized by a sharp 90° bend.

3.4 Vector Analysis of Sedimentation in Open Channels

The prediction of sediment deposition sites within an open channel can be achieved by examining the velocity vectors generated in a 3D simulation employing a CFD approach. Following the demonstration of the velocity field, the analysis extends to forecasting sediment deposition locations in open channels by scrutinizing the patterns of velocity vectors observed in straight, branched, and 90-degree curved channels. When analyzing the velocity vector and predicting sediment deposition locations across these channel types, it is crucial to observe the disparities evident at depths near the surface (h = 0.45 m) and near the channel bed (h = 0.05 m).

At a depth close to the surface, h = 0.45 m, the velocity vector at the center of the channel appears relatively high, characterized by elongated vector lines (Figure 6(a)). Conversely, at a depth near the channel bed, h = 0.05 m, the velocity vector noticeably diminishes, evident from the shorter vector lines (Figure 6(b)). This observation indicates that in straight channels, sedimentation sites are more likely to occur near the channel bed. This variation aligns with the scientific principle stating that flow velocities tend to decrease near the channel bed, thereby increasing the likelihood of sedimentation.

JOMAse | Received: 18-May-2024 | Accepted: 30-July-2924 | [(68) 2: 53-63]
Published by International Society of Ocean, Mechanical and Aerospace Scientists and Engineers, www.isomase.org., ISSN: 2354-7065 & e-ISSN: 2527-6085

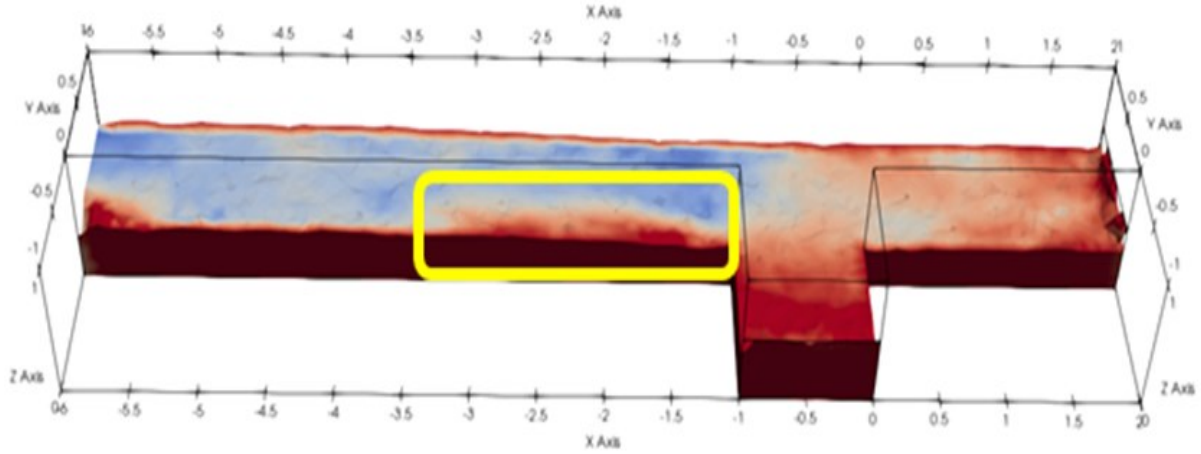

(a)

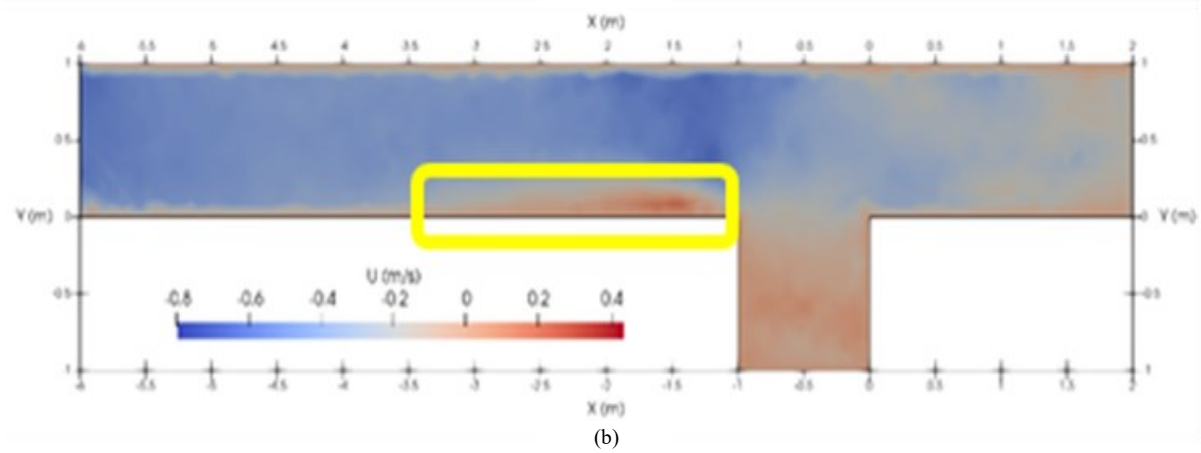

(b)

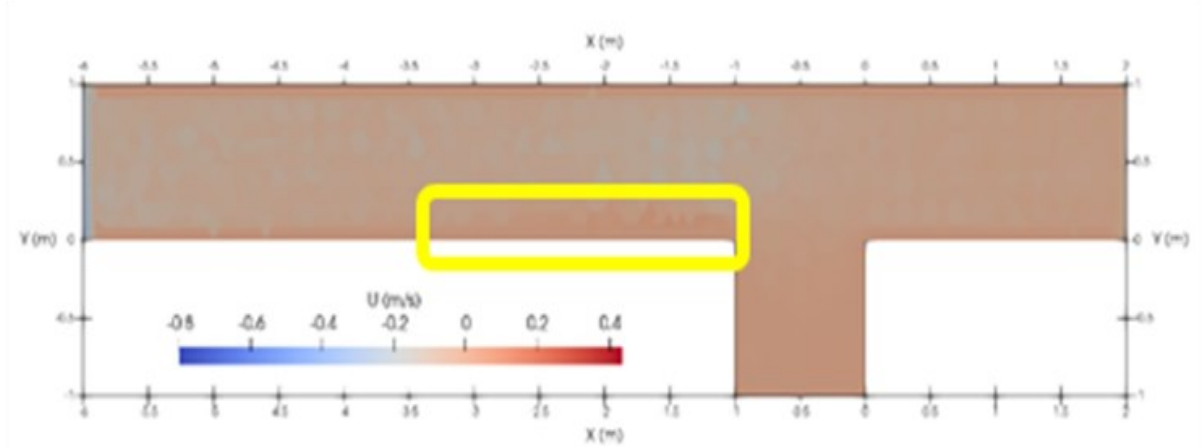

(c)

Figure 4: (a) 3D simulation illustrating water flow in a branched channel; Bird's-eye view: (a) in proximity to the surface at h = 0.45 m, and (b) close to the channel bed at h = 0.05 m.

JOMAse | Received: 18-May-2024 | Accepted: 30-July-2924 | [(68) 2: 53-63]
Published by International Society of Ocean, Mechanical and Aerospace Scientists and Engineers, www.isomase.org., ISSN: 2354-7065 & e-ISSN: 2527-6085

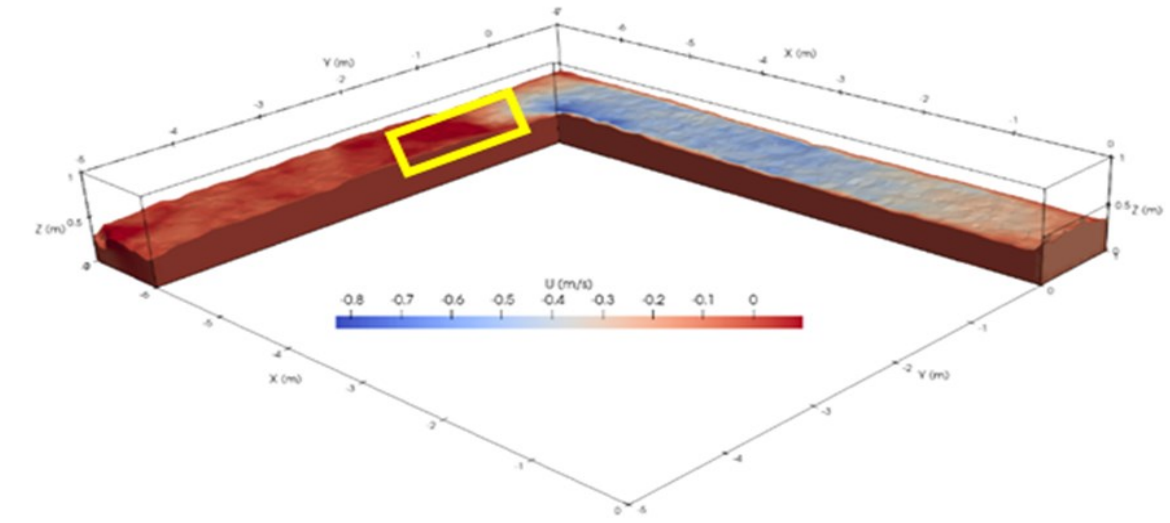

(a)

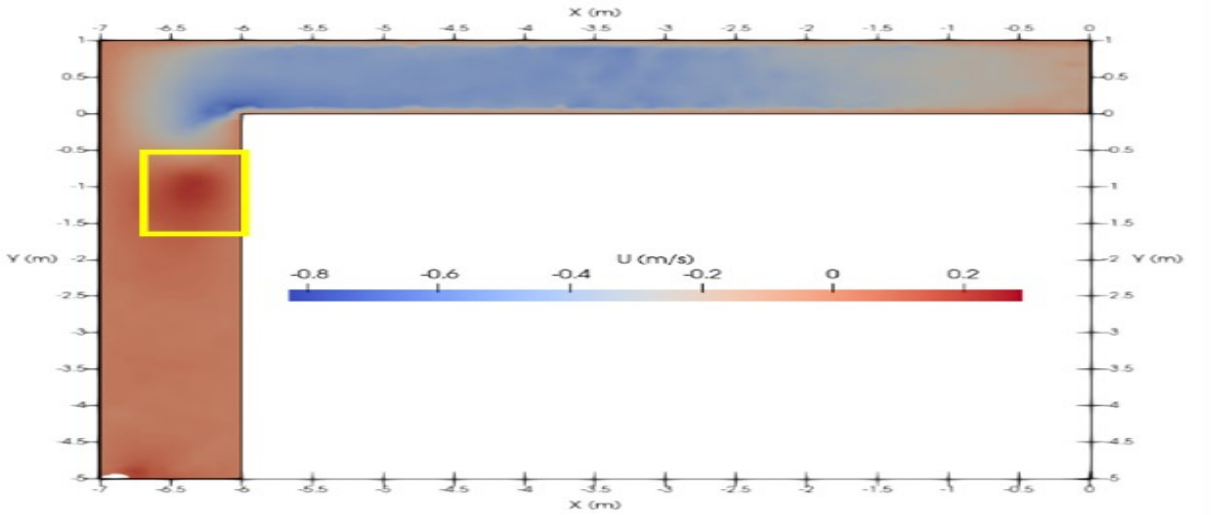

(b)

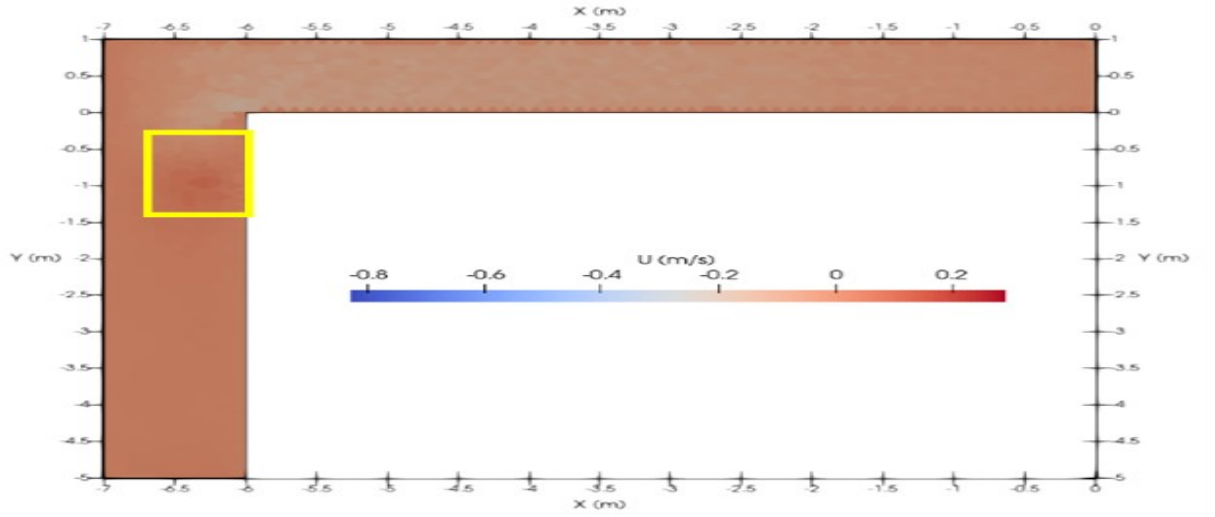

(c)

Figure 5: (a) 3D simulation depicting water flow in a 90° curved channel; Bird's-eye view, (b) at a proximity to the surface, h = 0.45m, and (c) close to the channel bed, h = 0.05 m

JOMAse | Received: 18-May-2024 | Accepted: 30-July-2924 | [(68) 2: 53-63]
Published by International Society of Ocean, Mechanical and Aerospace Scientists and Engineers, www.isomase.org., ISSN: 2354-7065 & e-ISSN: 2527-6085

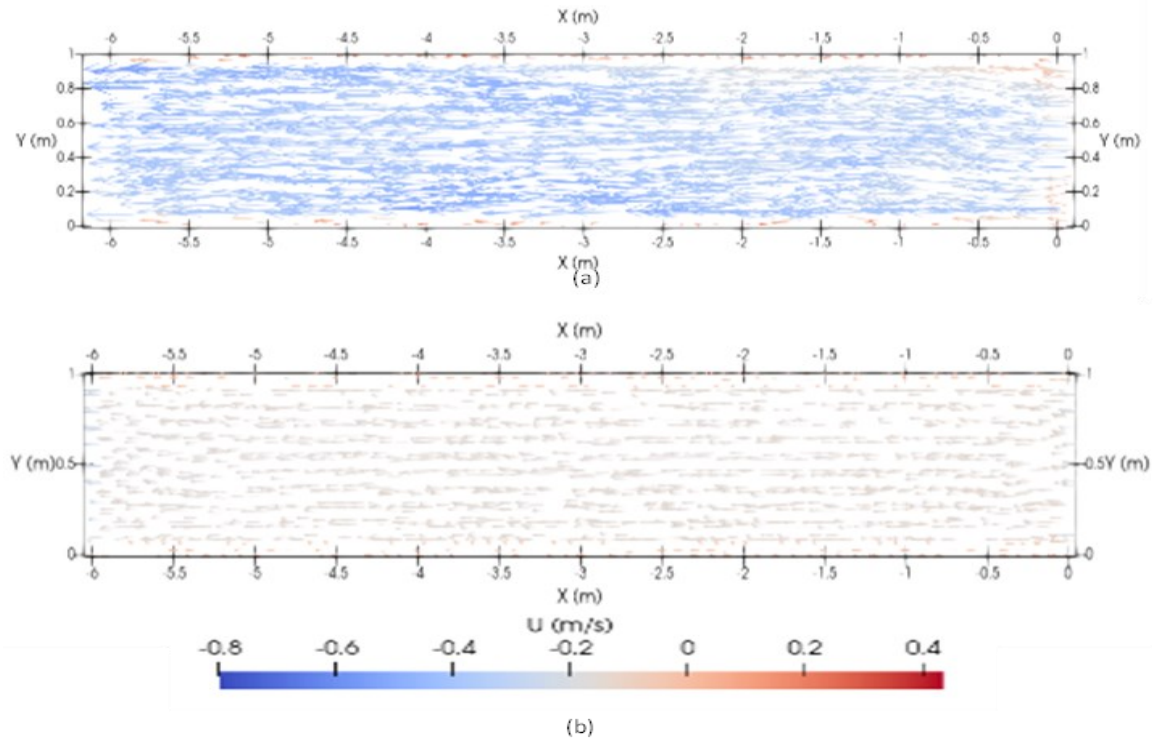

Figure 6: (a) Bird's-eye view of the velocity vectors in a linear channel: (a) proximity to the surface depth at h = 0.45 m, and (b) close to the channel bed depth at h = 0.05 m.

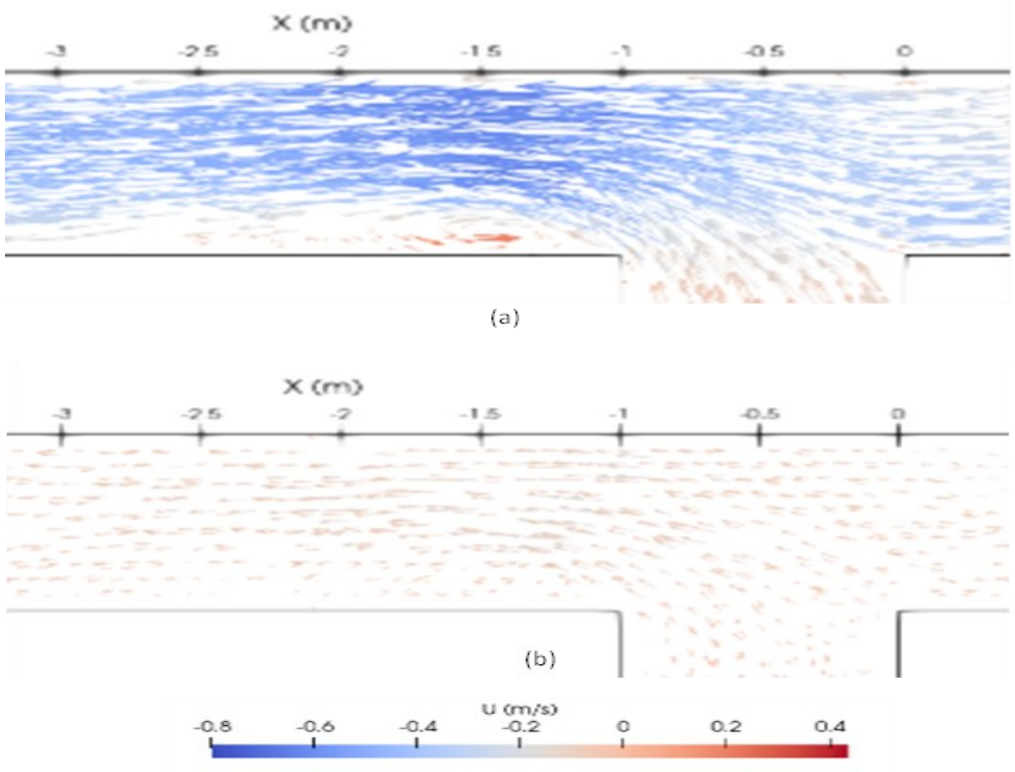

Figure 7: Bird's-eye view of the velocity vectors in a branched channel: (a) at a depth near the surface, h = 0.45 m, and (b) at a depth near the channel bed, h = 0.05 m.

JOMAse | Received: 18-May-2024 | Accepted: 30-July-2924 | [(68) 2: 53-63]
Published by International Society of Ocean, Mechanical and Aerospace Scientists and Engineers, www.isomase.org., ISSN: 2354-7065 & e-ISSN: 2527-6085

ISOMAse
International Society of Ocean, Mechanical and Aerospace Scientists and Engineers
Journal of Ocean, Mechanical and Aerospace
-Science and Engineering-
30th July 2024. Vol.68 No.2

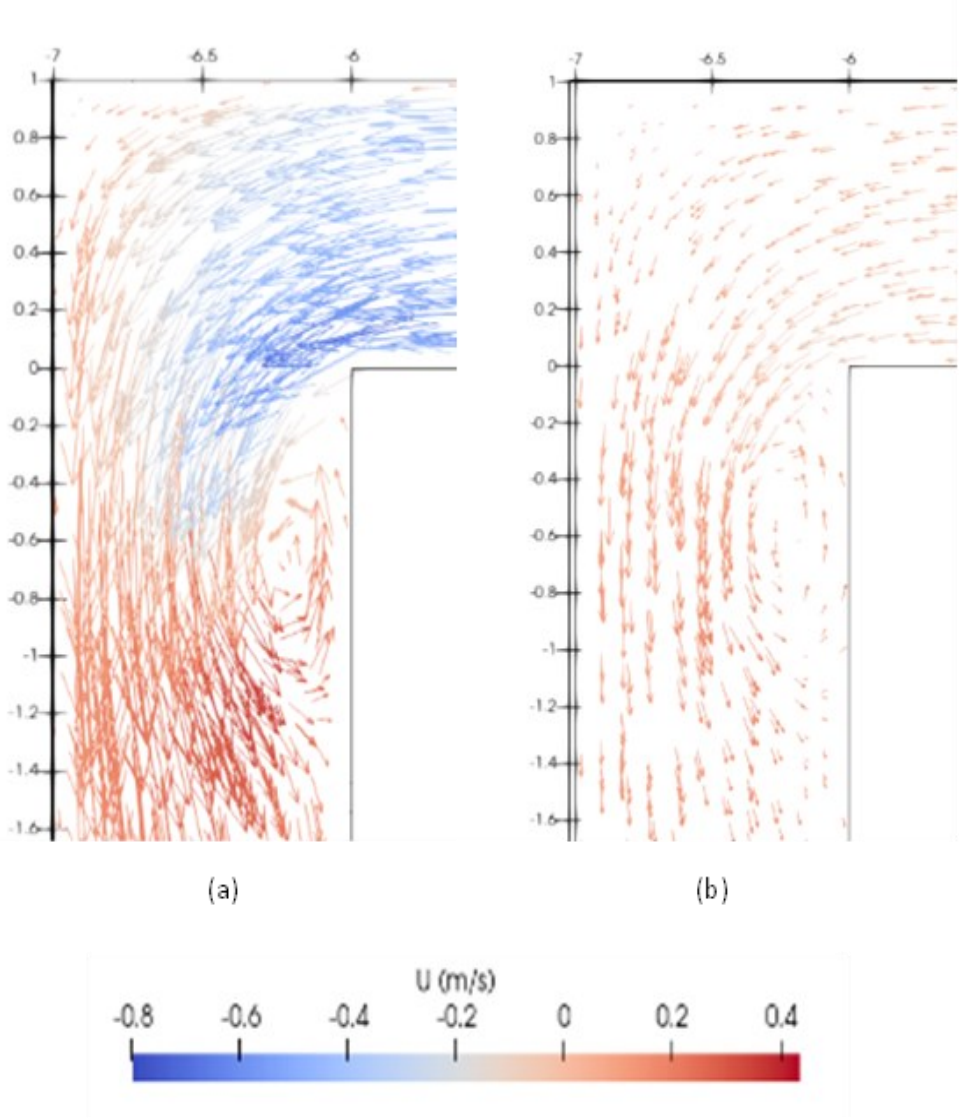

Figure 8: Bird's-eye view of the velocity vectors in a 90° curved channel: (a) proximity to the surface depth at h = 0.45 m, and (b) close to the channel bed depth at h = 0.05 m

In branched channels (Figure 7), the disparity between the depth near the surface and the channel bottom also impacts the velocity distribution. The water vortex following the channel bifurcation is evident at a depth near the surface, h = 0.45 m (Figure 7(a)). Similarly, at a depth near the channel bed, h = 0.05 m, this vortex becomes increasingly concentrated towards the bottom region (Figure 7(b)). This suggests that this area could serve as a sedimentation site due to the reduced velocity and the formation of water vortices.

Examination of the velocity vector field within a channel subjected to a sharp 90° bend at various depths uncovers a direct correlation between the velocity vector and the emergence of water eddies within the flow (Figure 8). At a depth close to the surface (h = 0.45 m), the velocity vector descends deeper into the channel, indicating a reduction in flow velocity (Figure 8(a)). On the outer side of the bend, the velocity vector ascends higher within the channel, signifying a velocity increase attributed to flow constriction. The alteration in velocity vector direction around a bend leads to the formation of a water vortex. Near the channel bed (h = 0.05 m), the eddies concentrate more towards the channel bottom, particularly on the inner bend (Figure 8(b)). The velocity vectors at this depth depict that the vortices arise due to the velocity differential between the flow's bottom and surface.

These whirlpools represent regions where the centrifugal force induced by a sharp bend causes a reduction in flow velocity near the channel bed. Consequently, sediment particles transported by the flow tend to accumulate in these regions owing to the decreased flow velocity. In simpler terms, these eddies serve as potential "catchments" for sediment within them. The correlation between the velocity vector and eddy formation holds significance in understanding sedimentation processes in channels featuring sharp bends. This underscores the importance of comprehending the interplay between water currents and channel bed morphology in forecasting sediment deposition sites across different flow scenarios.

JOMAse | Received: 18-May-2024 | Accepted: 30-July-2924 | [(68) 2: 53-63]
Published by International Society of Ocean, Mechanical and Aerospace Scientists and Engineers, www.isomase.org., ISSN: 2354-7065 & e-ISSN: 2527-6085

4.0 CONCLUSIONS

Validation studies indicate that 3D simulations employing a CFD approach with OpenFOAM software can accurately replicate velocity distribution within an open channel. These validation findings enhance confidence in the applicability of the CFD model for depicting water flow in open channels. Simulation outcomes incorporating branched channel configurations demonstrate that alterations in channel geometry can impact changes in water velocity. Notably, a decline in flow velocity is observed following the branching point of two channels, which holds implications for understanding sedimentation mechanisms, wherein reduced velocity can affect sediment particle settling patterns. Additionally, simulations of flow in a channel featuring a 90° bend reveal a notable decrease in flow velocity post-bend passage. This decline is attributed to centrifugal force effects stemming from flow direction alterations. Such findings bear significance in comprehending flow dynamics within channels characterized by sharp bends.

Analysis of velocity vectors in the simulation enables the anticipation of sediment deposition sites in open channels. Disparities in velocity between the surface and the channel bed depth dictate sedimentation locales. In linear channels, sedimentation tends to occur predominantly near the channel bed and along its edges. In branched channels, water whirlpools localize in the vicinity post-bifurcation and near the channel bed, earmarking these areas as potential sedimentation zones. Similarly, within a 90° curved channel, velocity reduction on the inner bend can generate whirlpools, serving as potential sediment traps.

Subsequent studies should delve into additional variables that might impact sedimentation mechanisms, such as diverse sediment compositions or fluctuations in initial flow velocities. Moreover, alternative turbulent models could be explored to gain a more profound comprehension of turbulence patterns affecting sediment dynamics. Integrating field experiments with CFD simulations in future research endeavors could furnish more holistic insights into sedimentation mechanisms within real-world scenarios. Hence, ongoing investigations aim to enhance our understanding of sedimentation mechanisms across diverse water flow scenarios in open channels.

ACKNOWLEDGEMENTS

We extend our sincere appreciation for the generous support and funding received through the DIPA Untan 2023 Grant, with reference to SP DIPA- 023.17.2.677517/2023, dated 30 November 2022, Contract No: 2662/UN22.8/PT.01.05/2023, which has been instrumental in facilitating this research. Furthermore, we would like to convey our gratitude for the provision of facilities by the Geophysics and GIS laboratories of the Geophysics Study Program, FMIPA Untan. These facilities have played a crucial role in conducting this research, enabling us to carry out the simulations and analyses effectively.

REFERENCES

[1] Kumbhakar, M., Tsai, C.W. & Absi, R. (2023). Semi-analytical modeling of sediment-laden open-channel flows with the effects of stratification, hindered settling, and eddy viscosities. *Chaos: An Interdisciplinary Journal of Nonlinear Science*, 33(8). doi: 10.1063/5.0157383.

[2] Kumbhakar, M. & Tsai, C.W. (2023). Analytical modeling of vertical distribution of streamwise velocity in open channels using fractional entropy. *Chaos Solitons Fractals*, 169, 113285. doi: 10.1016/j.chaos.2023.113285.

[3] Zahiri, A., Tang, X. & Dahanzadeh, B. (2022). A model for predicting the lateral distribution of sediment transport in river bends. *ISH Journal of Hydraulic Engineering*, 28(4), 420-429. doi: 10.1080/09715010.2021.1954100.

[4] Gounder Krishnappan, B. et al. (2020). Experimental investigation of erosion characteristics of fine-grained cohesive sediments. *Water (Basel)*, 12(5), 1511. doi: 10.3390/w12051511.

[5] Li, Y., Zhang, J., Xu, H. & Bai, Y. (2021). Experimental study on the characteristics of sediment transport and sorting in pressurized pipes. *Water (Basel)*, 13(19), 2782. doi: 10.3390/w13192782.

[6] Wang, X., Yan, X., Duan, H., Liu, X & Huang, E. (2019). Experimental study on the influence of river flow confluences on the open channel stage–discharge relationship. *Hydrological Sciences Journal*, 64(16), 2025-2039. doi: 10.1080/02626667.2019.1661415.

[7] Nazari-Giglou, A., Jabbari-Sahebari, A., Shakibaeinia, A. & Borghei, S.M. (2016). An experimental study of sediment transport in channel confluences. *International Journal of Sediment Research*, 31(1), 87-96. doi: 10.1016/j.ijsrc.2014.08.001.

[8] Chaudhary, H.P., Isaac, N., Tayade, S.B. & Bhosekar, V.V. (2019). Integrated 1D and 2D numerical model simulations for flushing of sediment from reservoirs. *ISH Journal of Hydraulic Engineering*, 25(1), 19-27. doi: 10.1080/09715010.2018.1423580.

[9] Jelti, S. & Boulerhcha, M. (2022). Numerical modeling of two-dimensional non-capacity model for sediment transport by an unstructured finite volume method with a new discretization of the source term. *Math Computer Simulation,* 197, 253-276. doi: 10.1016/j.matcom.2022.02.012.

[10] Arthur, J.K. (2023). PIV Measurements of open-channel turbulent flow under unconstrained conditions. *Fluids*, 8(4), 135. doi: 10.3390/fluids8040135.

[11] Yang, F., Shao, X., Fu, X. & Kazemi, E. (2019). Simulated flow velocity structure in meandering channels: stratification and inertia effects caused by suspended sediment. *Water (Basel)*, 11(6), 1254. doi: 10.3390/w11061254.

[12] Montaseri, H., Tavakoli, K., Evangelista, S. & Omidvar,

P. (2020). Sediment transport and bed evolution in a 180◦ curved channel with lateral intake: numerical simulations using eulerian and discrete phase models. *International Journal of Modern Physics C*, 31(08), 2050113. doi: 10.1142/S0129183120501132.

[13] Yang, Q.Y., Liu, T.H., Lu, W.Z. & Wang, X.K. (2013). Numerical simulation of confluence flow in open channel with dynamic meshes techniques. *Advances in Mechanical Engineering*, 5, 860431. doi: 10.1155/2013/860431.

[14] Esipov D. & Kuranakov, D. (2023). 2D CFD-DEM numerical simulation of the sedimentation of circular particles in the rectangular inclined vessel. 030011. doi: 10.1063/5.0132644.

[15] Mohammad, M.E., Al-Ansari, N., Knutsson, S. & Laue, J. (2020). A computational fluid dynamics simulation model of sediment deposition in a storage reservoir subject to water withdrawal. *Water (Basel)*, 12(4), 959. doi: 10.3390/w12040959.

[16] Charafi, M.M. (2019). Two-dimensional numerical modeling of sediment transport in a dam reservoir to analyze the feasibility of a water intake. *International Journal of Modern Physics C*, 30(01), 1950003. doi: 10.1142/S0129183119500037.

[17] Hu, L., Dong, Z., Peng, C. & Wang, L.P. (2021). Direct numerical simulation of sediment transport in turbulent open channel flow using the lattice boltzmann method. *Fluids*, 6(6), 217. doi: 10.3390/fluids6060217.

[18] Peng, C., Ayala, O.M. & Wang, L.P. (2020). Flow modulation by a few fixed spherical particles in a turbulent channel flow. *Journal Fluid Mechanic*, 884, A15. doi: 10.1017/jfm.2019.933.

[19] Duan, J.G., Yu, C. & Ding, Y. (2023). Numerical simulation of sediment transport in unsteady open channel flow. *Water (Basel)*, 15(14), 2576. doi: 10.3390/w15142576.

[20] Ben Hamza, S., Ben Kalifa, R., Saïd, N.M., Bournot, H. & Le Palec, G. (2017). Numerical study of sediment transport in turbulent two-phase flows around an obstacle. *Applied Math Model*, 45, 97-122. doi: 10.1016/j.apm.2016.12.021.

[21] Sahoo, A., Samantaray, S. & Singh, R.B. (2020). Analysis of velocity profiles in rectangular straight open channel flow. *Pertanika Journal. Science & Technology*, 28(1), 1-18.

[22] Akoz, M.S., Soydan, N.G. & Simsek, O. (2016) Numerical validation of open channel flow over a curvilinear broad-crested weir. P*rogress in Computational Fluid Dynamics, An International Journal*, 16(6), 364. doi: 10.1504/pcfd.2016.10000916.

[23] Alawadi, W., Prasad, T.D. & Al-Salih, O. (2019). Assessing the impact of velocity dip and wake coefficients on velocity prediction for open channel flows. *Research Journal of Applied Sciences, Engineering and Technology*, 16(1), 9-14, doi: 10.19026/rjaset.16.5993.

[24] Putra, Y.S., Beaudoin, A., Rousseaux, G., Thomas, L. & Huberson, S. (2019). 2D numerical contributions for the study of non-cohesive sediment transport beneath tidal bores. *Comptes Rendus Mécanique*, 347(2), 166-180. doi: 10.1016/j.crme.2018.11.004.

[25] Mirauda, D. & Russo, M.G. (2020). Entropy wake law for stream-wise velocity profiles in smooth rectangular open channels. *Entropy*, 22(6), 654. doi: 10.3390/e22060654.

[26] Mahananda, M., Hanmaiahgari, P.R., Ojha, C.S.P. & Balachandar, R. (2019). A new analytical model for dip modified velocity distribution in fully developed turbulent open channel flow. *Canadian Journal of Civil Engineering*, 46(8), 657-668. doi: 10.1139/cjce-2018-0615.

[27] Kumbhakar, M., Ghoshal, K. & Singh, V.P. (2020). Two-dimensional distribution of streamwise velocity in open channel flow using maximum entropy principle: Incorporation of additional constraints based on conservation laws. *Computer Methods Applied Mechanical Engineering*, 361, 112738. doi: 10.1016/j.cma.2019.112738.

[28] Mirauda D. & Russo, M.G. (2019). information entropy theory applied to the dip-phenomenon analysis in open channel flows. *Entropy*, 21(6), 554. doi: 10.3390/e21060554.

[29] Absi, R. (2011). An ordinary differential equation for velocity distribution and dip-phenomenon in open channel flows. *Journal of Hydraulic Research*, 49(1), 82-89. doi: 10.1080/00221686.2010.535700.

[30] Coles, D. (1956). The law of the wake in the turbulent boundary layer. *Journal of Fluid Mechanic*, 1(2), 191-226. doi: 10.1017/S0022112056000135.